# Quantum Phase Transition at Nonzero Doping in a Random *t-J* Model

Henry Shackleton[1], Alexander Wietek[2], Antoine Georges[2,3,4,5] and Subir Sachdev[1]

[1]*Department of Physics, Harvard University, Cambridge, Massachusetts 02138, USA*
[2]*Center for Computational Quantum Physics, Flatiron Institute, New York, New York 10010, USA*
[3]*Collège de France, 11 place Marcelin Berthelot, 75005 Paris, France*
[4]*CPHT, CNRS, École Polytechnique, IP Paris, F-91128 Palaiseau, France*
[5]*DQMP, Université de Genève, 24 quai Ernest Ansermet, CH-1211 Genève, Switzerland*

We present exact diagonalization results on finite clusters of a *t-J* model of spin-1/2 electrons with random all-to-all hopping and exchange interactions. We argue that such random models capture qualitatively the strong local correlations needed to describe the cuprates and related compounds, while avoiding lattice space group symmetry breaking orders. The previously known spin glass ordered phase in the insulator at doping $p = 0$ extends to a metallic spin glass phase up to a transition $p = p_c \approx 1/3$. The dynamic spin susceptibility shows signatures of the spectrum of the Sachdev-Ye-Kitaev models near $p_c$. We also find signs of the phase transition in the entropy, entanglement entropy, and compressibility, all of which exhibit a maximum near $p_c$. The electron energy distribution function in the metallic phase is consistent with a disordered extension of the Luttinger-volume Fermi surface for $p > p_c$, while this breaks down for $p < p_c$.

Two recent experiments [1,2] have shed new light on the transformation in the metallic parent state of the cuprate superconductors near optimal doping, while also highlighting the central theoretical puzzles. Angle-dependent magnetoresistance measurements in $La_{1.6-x}Nd_{0.4}Sr_xCuO_4$ [1] are compatible with a Luttinger-volume "large" Fermi surface only at a hole doping $p > p_c \approx 0.23$. Nuclear magnetic resonance and sound velocity measurements in $La_{2-x}Sr_xCuO_4$ [2] in high magnetic fields have uncovered glassy antiferromagnetic order for $p < p_c \approx 0.19$. These, and other, observations show that the parent metallic state of the cuprates exhibits Fermi liquid behavior for $p > p_c$, and transforms to an enigmatic pseudogap metal with glassy magnetic order for $p < p_c$. Observations also indicate that the reshaping of the Fermi surface, and the onset of the pseudogap, for $p < p_c$ cannot be explained by long-range antiferromagnetic order, which sets in at a doping smaller than $p_c$.

Here, we present exact diagonalization results on clusters of $N$ sites of a *t-J* model with random and all-to-all hopping and exchange interactions [see Eq. (1)]. In the thermodynamic limit $N \rightarrow \infty$, the replica-diagonal saddle point of this model and a related Hubbard model [3] are described by (extended) dynamic mean-field equations in which the disorder self-averages [4]. Moreover, closely related mean-field equations also appear in nonrandom models in high spatial dimensions [9,10], indicating that the self-averaging features of the random models properly capture generic aspects of strong correlation physics. A direct solution of the $N = \infty$ replica-diagonal saddle point of the Hubbard model is presented in a separate paper [11],

with complementary results which are consistent with our conclusions below.

The insulating model at $p = 0$ has been studied previously by exact diagonalization [12], and a non-self-averaging spin glass ground state was found. We find similar results at $p = 0$, but with a reduced estimate for the magnitude of the spin glass Edwards-Anderson order parameter $q$. At nonzero $p$, we find that $q$ decreases monotonically, vanishing at a quantum phase transition $p_c \approx 1/3$. We present several results for thermodynamic, entanglement, and spectral properties across this transition. All our results are consistent with the presence of a self-averaging Fermi liquid state for $p > p_c$; in particular, we find that the one-particle energy distribution function is consistent with a disordered analog of the Luttinger theorem [4]. The entropy, entanglement entropy, and compressibility all have maxima near $p_c$. We find that the low-frequency dynamic spin susceptibility matches that of the Sachdev-Ye-Kitaev (SYK) class of models [13,14] over a significant range of frequencies near $p_c$; this includes a subleading contribution which arises from a boundary graviton in dual models of two-dimensional quantum gravity [15–19]. Such spectral features are not present in theories that treat the transition at $p = p_c$ in a Landau-Ginzburg-Hertz framework for the onset of spin glass order in a Fermi liquid [20,21].

*Random t-J model.*—We consider the Hamiltonian,

$$H = \frac{1}{\sqrt{N}} \sum_{i \neq j=1}^{N} t_{ij} P c_{i\alpha}^\dagger c_{j\alpha} P + \frac{1}{\sqrt{N}} \sum_{i < j=1}^{N} J_{ij} \mathbf{S}_i \cdot \mathbf{S}_j, \quad (1)$$
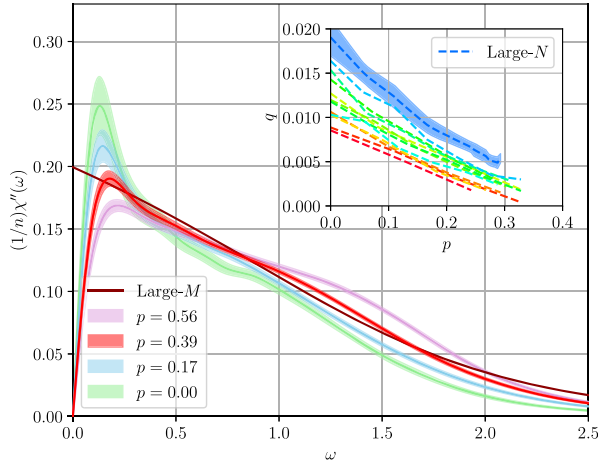
FIG. 1. The spectral function $\chi''(\omega)$ of the random $t$-$J$ model, averaged over 100 disorder realizations on an 18-site cluster. At low dopings, a sharp peak at low frequency at low doping is indicative of spin glass order. With increasing doping, the magnitude of this peak is reduced, and the low-frequency behavior closely resembles the rescaled spectral function of the large-$M$ SYK theory [13,18,19]. Inset: After an extrapolation to the thermodynamic limit, the integrated weight of the low-frequency peak is nonzero, indicating spin glass order. This weight vanishes near $p \approx 0.4$. Plotted is the integrated weight for $8 \leq N \leq 18$ (as a gradient from red to blue) and the large-$N$ extrapolation with error bars.

where $P$ is the projection on nondoubly occupied sites and $\mathbf{S}_i = (1/2)c_{i\alpha}^\dagger \boldsymbol{\sigma}_{\alpha\beta} c_{i\beta}$ is the spin operator on site $i$. The hoppings $t_{ij} = t_{ji}^*$ and real exchange interactions $J_{ij}$ are independent random numbers with zero mean and variance $t^2$, $J^2$. Henceforth, we set $t = J = 1$. We work in the canonical ensemble, where our system has a fixed particle (hole) density, $n$ ($p = 1 - n$). At $p = 0$, hopping is prevented due to the double occupancy constraint, and the model reduces to an infinite-range Heisenberg model with random couplings. The $p = 0$ model has been studied analytically by generalizing the $SU(2)$ symmetry to $SU(M)$ and taking a large-$M$ limit [13,22,23], and numerically for the case of $M = 2$ [12,24]. For $SU(2)$, a spin glass phase is found below a critical temperature $T_c \approx 0.10J$. When doping is present, Ref. [25] predicts a disordered Fermi liquid phase for all nonzero values of $p$ in the large-$M$ limit. However, it was recently argued [26,27] that for the case of $SU(2)$, the spin glass phase should persist up to a critical finite value of doping $p_c$ corresponding to a quantum critical point separating the spin glass phase from a disordered Fermi liquid. Near criticality, the model is predicted to exhibit SYK-like criticality with a nonzero extensive entropy and a linear-in-temperature resistivity [28]. In a weak-coupling renormalization group, this critical point emerges when the three fractionalized excitations in the $t$-$J$ model become degenerate in energy, leading to a zeroth order prediction of $p_c = 1/3$.

*Dynamical spin response at $T = 0$.*—We first present results on the nature of the spin correlations at $T = 0$, providing evidence that the spin glass phase shown to exist at $p = 0$ is stable for small values of doping, up to a critical value of doping near $p = 1/3$. Using the Lanczos algorithm, we calculate the spectral function at $T = 0$,

$$\chi''(\omega) = \frac{1}{3}\sum_\alpha \frac{1}{N}\sum_i \sum_n |\langle\psi_n|S_i^\alpha|\psi_0\rangle|^2$$
$$\times [\delta(\omega - (E_n - E_0)) - \delta(\omega + (E_n - E_0))], \quad (2)$$

where numerically the $\delta$ functions are replaced by Gaussians with a small variance. The signature of spin glass order, $\lim_{t\to\infty}(1/N)\sum_i\langle\mathbf{S}_i(0)\mathbf{S}_i(t)\rangle = q \neq 0$, is reflected by a $q\delta(\omega)$ contribution to the dynamical structure factor $S(\omega)$, which is related to the spectral function at $T = 0$ by $\chi''(\omega) = S(\omega) - S(-\omega)$. For a finite system size, the exact $\delta$ function in $S(\omega)$ is replaced by a peak at low frequency, whose width approaches 0 in the thermodynamic limit and whose total spectral weight gives $q$. Therefore, the spin glass contribution to $\chi''(\omega)$ for finite systems is given by a low-frequency peak, and was analyzed for this model at $p = 0$ in Ref. [12]. Above $p_c$, a disordered Fermi liquid is expected to have a low-frequency behavior of $\chi''(\omega) \sim \omega$.

The spectral function for the random $t$-$J$ model, calculated using the Lanczos algorithm on an 18-site cluster, is shown for several values of doping in Fig. 1. A prominent hump at low frequency for dopings $p \lesssim 0.4$ suggests the presence of spin glass order in this range of doping. However, a large-$N$ analysis of this hump must be performed in order to verify that the hump asymptotes to a $\delta$ function in the thermodynamic limit. To do this, we first subtract off a background contribution to account for the rest of the spectral weight. Anticipating SYK behavior near the critical point at low frequencies, we subtract a spectral weight obtained by rescaling the solution of the Schwinger-Dyson equations of the $p = 0$ model in the large-$M$ limit [13,18,19] (we rescale $J$, while preserving total spectral weight). This SYK spectral weight has a leading term $\chi''(\omega) \sim \text{sgn}(\omega)$ as $|\omega| \to 0$ at $T = 0$ [which generalizes to $\tanh(\omega/2T)$ at low $T$]. The next-to-leading SYK term depends linearly in $\omega$, and arises from the boundary graviton in the holographic dual [18,19]. It is important to note that the exponents of these two leading SYK contributions are universal and independent of $M$. Away from the critical point and in the spin glass phase, we find that the spectral function is described well by a combination of the SYK result and a low-frequency hump. A large-$N$ analysis of this low-frequency hump, described in more detail in the Supplemental Material [4], confirms that the variance of the hump vanishes in the thermodynamic limit, whereas the spectral weight, shown in Fig. 1, remains nonzero. Our analysis gives a large-$N$ estimate of $q \sim 0.02$ at $p = 0$. For larger values of doping,

$q$ decreases from its value at $p = 0$, eventually vanishing at some critical value of doping $p_c$. By linearly extrapolating the large-$N$ prediction for $q$ to higher dopings, we obtain an estimate of $p_c = 0.420 \pm 0.007$. Around this range of dopings, the spectral function shows good agreement with the large-$M$ critical prediction given in Fig. 1. At dopings well above $p = 0.4$, we find the spectral function to be largely independent of system size. No gap at low frequency is visible, and $\chi''(\omega) \sim \omega$ behavior consistent with Fermi liquid predictions is clear. We will provide a more rigorous verification of the Fermi liquid phase at higher dopings via Luttinger's theorem later in the Letter.

*Thermodynamics and entanglement.*—We investigate the specific heat and thermal entropy given by

$$C = \frac{\partial E}{\partial T} \quad \text{and} \quad S = \log(\mathcal{Z}) + \frac{E}{T}, \quad (3)$$

where $\mathcal{Z}$ denotes the canonical partition function and $E = \langle H \rangle$ the internal energy. Results for system sizes $N = 12, 16, 18$ are shown in Fig. 2. To obtain the results on system sizes $N = 16, 18$ we employed thermal pure quantum (TPQ) states [29,30] as described in Refs. [31–33] similar to the finite-temperature Lanczos method [34,35] (see Ref. [4] for details). For each set of random couplings, we sampled $R = 5$ TPQ states, cf. Ref. [32]. Error estimates have been obtained from 1000 (400, 100) random couplings for $N = 12$ (16, 18).

The specific heat for $p = 0$ in Fig. 2(a) exhibits a broad maximum at $T \approx 0.25$, in agreement with previous results [12]. At small values of doping $p \lesssim 1/6$, this maximum remains at $T \approx 0.25$, while we observe an increase of the specific heat at higher temperatures. The maximum is gradually shifted toward a higher value $T \approx 0.50$ for dopings from $p = 1/4$ to $p = 1/2$. At low temperatures we observe that the specific heat is approximately linear in temperature, with a maximal slope attained between dopings $p = 0.20$ and $p = 0.40$. The linear-in-$T$ coefficient of the specific heat, $\gamma = C/T$, is shown in Fig. 2(b).

We observe an increase of $\gamma$ when lowering the temperature for all values of doping. We show $\gamma$ at temperature $T = 0.05$ as a function of doping in Fig. 2(c) for $N = 12, 16, 18$. At this temperature, the maximum is attained at $p \approx 0.25$. However, we find that this maximum is dependent on the temperature. At temperatures below $T = 0.05$ sample fluctuations become too large for a reliable estimate of the maximum. We note that a divergence of the $\gamma$ coefficient has been reported at the pseudogap quantum critical point in cuprate superconductors [36].

The thermal entropy for different temperatures and $N = 12, 16, 18$ is shown in Fig. 2(d). Again we observe maxima at dopings between $p = 0.20$ and $p = 0.40$ depending on temperature. At $T = 0.05$ the maximum is attained at

$$\tilde{p} \approx 0.296 \pm 0.025. \quad (4)$$

We refer to the Supplemental Material [4] for more discussion of the $T$ dependence of the thermal entropy. To access the limit $T \rightarrow 0$ we calculate the von Neumann entanglement entropy of the ground state:

$$\mathcal{S}_{vN}(A) = -\text{Tr}[\rho_A \log \rho_A]. \quad (5)$$

Here, $\rho_A = \text{Tr}_B(|\psi_0\rangle \langle \psi_0|)$ is the reduced density matrix of the ground state $|\psi_0\rangle$ on a subsystem $A$. $B$ denotes the complement of $A$. Results for $\mathcal{S}_{vN}(A)$ for subsystem sizes $M = 1, 2, 3, 4$ and total system sizes $N = 10, 12, 16$ are shown in Fig. 3. We find that the single-site ($M = 1$) and two-site ($M = 2$) entanglement entropy are well converged as a function of total system size $N$. For a $N = 16$ site cluster and $M = 4$ we estimate the maximum to be located at

$$\tilde{p} \approx 0.285 \pm 0.024 \quad [\text{from}\mathcal{S}_{vN}(A)], \quad (6)$$

in agreement with our estimate obtained from the thermal entropy at $T = 0.05$ in Eq. (4).



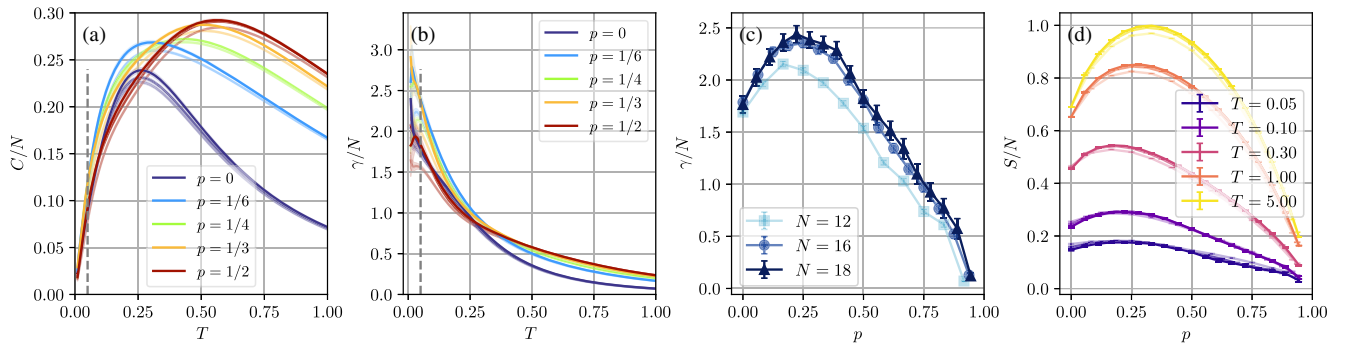FIG. 2. Thermodynamics of the random $t$-$J$ model for system sizes $N = 12, 16, 18$, indicated by increasing opacity. (a) The specific heat $C$ as a function of temperature for various values of doping. (b) The linear-in-$T$ coefficient of specific heat, $\gamma = C/T$, for various dopings as a function of temperature, and (c) for $T = 0.05$ as a function of doping. (d) The thermal entropy $S$ as a function of doping for various temperatures.
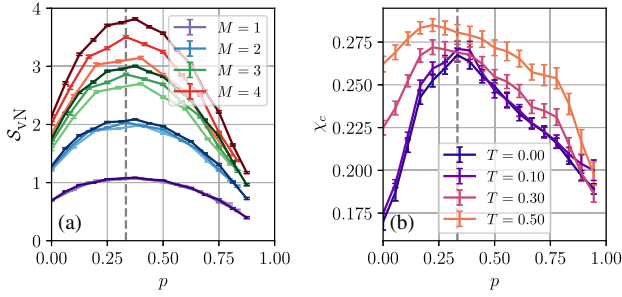
FIG. 3. (a) The ground state entanglement entropy $\mathcal{S}_{vN}$ of subsystems of size $M$. Results are compared for total system size $N = 10$, 12, 16, shown as increasing opacity. The maxima are attained at values close to $p = 1/3$, indicated by the gray dashed line. (b) Charge susceptibility $\chi_c$ for different temperatures at $N = 18$. The low-temperature maximum at doping $p = 1/3$ is shifted toward a smaller doping $p \approx 0.2$ at higher temperatures.

Finally, we investigate the charge susceptibility (compressibility),

$$\chi_c = \frac{\partial n}{\partial \mu} = \left( \frac{\partial^2 e}{\partial n^2} \right)^{-1} = \left( \frac{\partial^2 e}{\partial p^2} \right)^{-1}, \qquad (7)$$

computed by taking the inverse of the second derivative of the internal state energy density $e = E/N$ with respect to doping $p$. Here, the chemical potential is given by $\mu = \partial e/\partial n$. Results for different temperatures at $N = 18$ are shown in Fig. 3(b). At temperatures $T = 0$ and $T = 0.1$ we detect a maximum at doping $p = 1/3$. We observe a shoulderlike feature at lower doping. At higher temperatures $T = 0.3$ and $T = 0.5$ this feature develops into a maximum at $p \approx 0.2$. We notice that this shift matches the shift of $\tilde{p}$ in the thermal entropy shown in Figs. 2(b) and 2(c). We note that the occurrence of a maximum in the compressibility, specific heat coefficient, and local entanglement entropy has been recently discussed in cluster-dynamical mean field theory studies of the Hubbard model without randomness in relation to the pseudogap and Mott critical points [37–40].

*Luttinger's theorem.*—Having found strong signatures of a spin glass phase persisting from half filling up to $p_c \approx 1/3$, we now provide evidence of a Fermi liquid phase at higher values of doping, which vanishes at a critical value of doping near the onset of spin glass order. To verify the presence of a Fermi liquid phase, we introduce the one-particle energy distribution function,

$$\mathcal{N}(\epsilon) = \frac{1}{N} \sum_\lambda \delta(\epsilon - \epsilon_\lambda) \sum_{ij\sigma} \langle \lambda | i \rangle \langle c_{i\sigma}^\dagger c_{j\sigma} \rangle \langle j | \lambda \rangle, \qquad (8)$$

where $|\lambda\rangle$ are the single-particle *noninteracting* eigenstates with energy $\epsilon_\lambda$, obtained by diagonalizing the hopping matrix $t_{ij}$. This quantity is analogous to the particle occupation number in momentum space $n(\mathbf{k})$ commonly
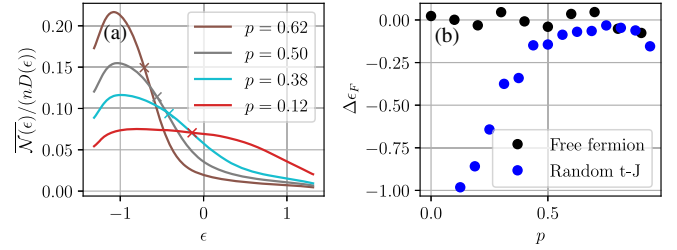


FIG. 4. (a) At high values of doping, the one-particle energy distribution function drops sharply near the energy level predicted by Luttinger's theorem (marked by crosses). At lower values of doping, this function becomes more broadened, suggesting a breakdown of Luttinger's theorem. (b) A comparison of the Fermi energy given by Luttinger's theorem and the numerically computed value given by the inflection point of the one-particle energy distribution function. For a 16-site cluster, the two show good agreement up to a critical value between $6/16 = 0.38$ and $7/16 = 0.44$, in contrast with the same quantity computed for free fermions which agree well for all values of doping.

used in systems with translational invariance. For a non-interacting system with fixed particle number $n$, the averaged quantity $\overline{\mathcal{N}(\epsilon)}$ converges to $D(\epsilon)\theta(\epsilon - \epsilon_F)$, where $D(\epsilon)$ is the single-particle density of states and $\epsilon_F$ is the Fermi energy, defined by

$$D(\epsilon) = \frac{1}{N} \overline{\sum_\lambda \delta(\epsilon - \epsilon_\lambda)}, n = 2 \int_{-\infty}^{\epsilon_F} d\epsilon D(\epsilon). \qquad (9)$$

For the interacting system, we show in the Supplemental Material [4] that, because the random couplings are all to all, $\mathcal{N}(\epsilon)$ displays self-averaging properties in the thermodynamic limit $N \to \infty$. In this limit, the signature of Luttinger's theorem is a discontinuity of $\overline{\mathcal{N}(\epsilon)}$ at the noninteracting value of $\epsilon_F$ defined in Eq. (9).

In Fig. 4, we plot the quantity $\overline{\mathcal{N}(\epsilon)}/D(\epsilon)$, averaged over 1000 realizations on a 16-site cluster. The density of states $D(\epsilon)$ is a semicircle distribution in the large-$N$ limit; however, in order to account for finite-size corrections to this distribution, we instead use the numerically calculated value of $D(\epsilon)$ obtained from our data. Although the drop in particle occupation at the Fermi energy is substantially broadened due to interactions and finite-size effects, the location of the inflection point still reliably tracks the location of the Fermi energy predicted by Luttinger's theorem at high values of doping as shown in Fig. 4. The effects of the infinite-strength Hubbard repulsion becomes stronger at lower values of doping, eventually causing a breakdown of Luttinger's theorem at a critical doping $0.38 < p_c < 0.44$, which is also the location where spin glass order appears to emerge.

*Discussion and conclusion.*—Our numerical results demonstrate a transition in the random all-to-all *t-J* model from a spin glass to a disordered Fermi liquid at a critical value of doping. The near-critical behavior has similarities

to the criticality of SYK models, consistent with recent theoretical proposals [26] and numerical results on related systems [3]. We find a near-critical dynamic spin susceptibility which is consistent with the SYK behavior $\chi''(\omega) \sim \text{sgn}(\omega)[1 - g|\omega| + \cdots]$ over a significant frequency regime; the $g$ term is a universal boundary "graviton" contribution. This is the first appearance of such features in a doped spin-1/2 SU(2) model. SYK criticality also predicts an extensive zero temperature entropy: we do find a maximum in the entropy near the critical point, but our finite-size data do not allow us to identify if there is an extensive contribution. However, we note that for SU($M = 2$) models, SYK criticality is preempted at small enough $T$ by a spin glass instability [11,23], and so the extensive $T = 0$ entropy is not ultimately expected. We also find a maximum in the entanglement entropy, specific heat coefficient, and compressibility near criticality.

An interesting observation is that the breakdown of Luttinger's theorem coming from high doping, as well as the vanishing of spin glass order from low doping, occurs near $p = 0.4$, which differs from the maxima in the thermodynamic and entanglement entropy closer to $p = 0.3$. While the system sizes accessible to our methods are relatively small and only discrete values of doping are accessible, recent extended dynamical mean field thoery calculations of the $t$-$J$ model with finite Hubbard repulsion [11] also give evidence of SYK criticality occurring at a lower value of doping than the spin glass-Fermi liquid transition. These observations are consistent with the spin glass instability of SYK criticality for finite $M$ [23] noted above. Understanding the nature of this separation, and the very low $T$ at which the spin glass instability of SYK criticality appears, remain open questions to be explored.

H. S. and A. W. contributed equally to this work.

———

[1] Y. Fang, G. Grissonnanche, A. Legros, S. Verret, F. Laliberte, C. Collignon, A. Ataei, M. Dion, J. Zhou, D. Graf, M. J. Lawler, P. Goddard, L. Taillefer, and B. J. Ramshaw, Fermi surface transformation at the pseudogap critical point of a cuprate superconductor, arXiv:2004.01725.

[2] M. Frachet, I. Vinograd, R. Zhou, S. Benhabib, S. Wu, H. Mayaffre, S. Krämer, S. K. Ramakrishna, A. P. Reyes, J. Debray, T. Kurosawa, N. Momono, M. Oda, S. Komiya, S. Ono, M. Horio, J. Chang, C. Proust, D. LeBoeuf, and M.-H. Julien, Hidden magnetism at the pseudogap critical point of a cuprate superconductor, Nat. Phys. **16,** 1064 (2020).

[3] P. Cha, N. Wentzell, O. Parcollet, A. Georges, and E.-A. Kim, Linear resistivity and Sachdev-Ye-Kitaev (SYK) spin liquid behavior in a quantum critical metal with spin-1/2 fermions, Proc. Natl. Acad. Sci. U.S.A. **117,** 18341 (2020).

[4] See Supplemental Material at http://link.aps.org/supplemental/10.1103/PhysRevLett.126.136602 for details of our analyses of the spin glass and disordered Fermi liquid phases, which includes Refs. [5–8].

[5] K. Levenberg, A method for the solution of certain non-linear problems in least squares, Q. Appl. Math. **2,** 164 (1944).

[6] D. W. Marquardt, An algorithm for least-squares estimation of nonlinear parameters, J. Soc. Ind. Appl. Math. **11,** 431 (1963).

[7] B. Efron and C. Stein, The jackknife estimate of variance, Ann. Stat. **9,** 586 (1981).

[8] A. Georges, G. Kotliar, W. Krauth, and M. J. Rozenberg, Dynamical mean-field theory of strongly correlated fermion systems and the limit of infinite dimensions, Rev. Mod. Phys. **68,** 13 (1996).

[9] J. L. Smith and Q. Si, Spatial correlations in dynamical mean-field theory, Phys. Rev. B **61,** 5184 (2000).

[10] K. Haule, A. Rosch, J. Kroha, and P. Wölfle, Pseudogaps in an Incoherent Metal, Phys. Rev. Lett. **89,** 236402 (2002).

[11] A. Dumitrescu, N. Wentzell, A. Georges, and O. Parcollet, Planckian metal at a doping-induced quantum critical point, arXiv:2103.08607.

[12] L. Arrachea and M. J. Rozenberg, Infinite-range quantum random Heisenberg magnet, Phys. Rev. B **65,** 224430 (2002).

[13] S. Sachdev and J. Ye, Gapless Spin-Fluid Ground State in a Random Quantum Heisenberg Magnet, Phys. Rev. Lett. **70,** 3339 (1993).

[14] A. Y. Kitaev, Entanglement in Strongly-Correlated Quantum Matter KITP, University of California, Santa Barbara (2015), https://online.kitp.ucsb.edu/online/entangled15/kitaev/.

[15] S. Sachdev, Holographic Metals and the Fractionalized Fermi Liquid, Phys. Rev. Lett. **105,** 151602 (2010).

[16] J. Maldacena and D. Stanford, Remarks on the Sachdev-Ye-Kitaev model, Phys. Rev. D **94,** 106002 (2016).

[17] A. Kitaev and S. J. Suh, The soft mode in the Sachdev-Ye-Kitaev model and its gravity dual, J. High Energy Phys. 05 (2018) 183.

[18] M. Tikhanovskaya, H. Guo, S. Sachdev, and G. Tarnopolsky, Excitation spectra of quantum matter without quasiparticles I: Sachdev-Ye-Kitaev models, Phys. Rev. B **103,** 075141 (2021).

[19] M. Tikhanovskaya, H. Guo, S. Sachdev, and G. Tarnopolsky, Excitation spectra of quantum matter without quasiparticles II: Random $t$-$J$ models, Phys. Rev. B **103,** 075142 (2021).

[20] A. M. Sengupta and A. Georges, Non-Fermi-liquid behavior near a $T = 0$ spin-glass transition, Phys. Rev. B **52,** 10295 (1995).

[21] S. Sachdev, N. Read, and R. Oppermann, Quantum field theory of metallic spin glasses, Phys. Rev. B **52,** 10286 (1995).

[22] A. Georges, O. Parcollet, and S. Sachdev, Mean Field Theory of a Quantum Heisenberg Spin Glass, Phys. Rev. Lett. **85**, 840 (2000).

[23] A. Georges, O. Parcollet, and S. Sachdev, Quantum fluctuations of a nearly critical Heisenberg spin glass, Phys. Rev. B **63**, 134406 (2001).

[24] A. Camjayi and M. J. Rozenberg, Quantum and Thermal Fluctuations in the SU($N$) Heisenberg Spin-Glass Model near the Quantum Critical Point, Phys. Rev. Lett. **90**, 217202 (2003).

[25] O. Parcollet and A. Georges, Non-Fermi-liquid regime of a doped Mott insulator, Phys. Rev. B **59**, 5341 (1999).

[26] D. G. Joshi, C. Li, G. Tarnopolsky, A. Georges, and S. Sachdev, Deconfined Critical Point in a Doped Random Quantum Heisenberg Magnet, Phys. Rev. X **10**, 021033 (2020).

[27] G. Tarnopolsky, C. Li, D. G. Joshi, and S. Sachdev, Metal-insulator transition in a random Hubbard model, Phys. Rev. B **101**, 205106 (2020).

[28] H. Guo, Y. Gu, and S. Sachdev, Linear in temperature resistivity in the limit of zero temperature from the time reparameterization soft mode, Ann. Phys. (Amsterdam) **418**, 168202 (2020).

[29] S. Sugiura and A. Shimizu, Thermal Pure Quantum States at Finite Temperature, Phys. Rev. Lett. **108**, 240401 (2012).

[30] S. Sugiura and A. Shimizu, Canonical Thermal Pure Quantum State, Phys. Rev. Lett. **111**, 010401 (2013).

[31] A. Wietek and A. M. Läuchli, Sublattice coding algorithm and distributed memory parallelization for large-scale exact diagonalizations of quantum many-body systems, Phys. Rev. E **98**, 033309 (2018).

[32] A. Wietek, P. Corboz, S. Wessel, B. Normand, F. Mila, and A. Honecker, Thermodynamic properties of the Shastry-Sutherland model throughout the dimer-product phase, Phys. Rev. Research **1**, 033038 (2019).

[33] A. Honecker, J. Richter, J. Schnack, and A. Wietek, Loop-gas description of the localized-magnon states on the kagome lattice with open boundary conditions, Condens. Matter Phys. **23**, 43712 (2020).

[34] J. Jaklič and P. Prelovšek, Lanczos method for the calculation of finite-temperature quantities in correlated systems, Phys. Rev. B **49**, 5065 (1994).

[35] P. Prelovšek and J. Bonča, *Ground state and finite temperature Lanczos methods*, in Strongly Correlated Systems: Numerical Methods, edited by A. Avella and F. Mancini (Springer, Berlin, 2013), pp. 1–30.

[36] B. Michon, C. Girod, S. Badoux, J. Kačmarčík, Q. Ma, M. Dragomir, H. A. Dabkowska, B. D. Gaulin, J. S. Zhou, S. Pyon, T. Takayama, H. Takagi, S. Verret, N. Doiron-Leyraud, C. Marcenat, L. Taillefer, and T. Klein, Thermodynamic signatures of quantum criticality in cuprate superconductors, Nature (London) **567**, 218 (2019).

[37] L. Fratino, P. Sémon, G. Sordi, and A. M. S. Tremblay, An organizing principle for two-dimensional strongly correlated superconductivity, Sci. Rep. **6**, 22715 (2016).

[38] G. Sordi, C. Walsh, P. Sémon, and A. M. S. Tremblay, Specific heat maximum as a signature of Mott physics in the two-dimensional Hubbard model, Phys. Rev. B **100**, 121105 (R) (2019).

[39] C. Walsh, P. Sémon, D. Poulin, G. Sordi, and A. M. S. Tremblay, Local Entanglement Entropy and Mutual Information across the Mott Transition in the Two-Dimensional Hubbard Model, Phys. Rev. Lett. **122**, 067203 (2019).

[40] C. Walsh, P. Sémon, D. Poulin, G. Sordi, and A.-M. S. Tremblay, Entanglement and classical correlations at the doping-driven Mott transition in the two-dimensional Hubbard model, PRX Quantum **1**, 020310 (2020).